Science and Technology Indonesia
e-ISSN:2580-4391 *p*-ISSN:2580-4405
Vol. 10, No. 4, October 2025

Research Paper

Precision Engineered Graphene Oxide Membranes Optimizing Thin Film Composite Layers for Solvent and Dye Separation

Januar Widakdo[1*], Fadly Azril Priodani[1,5], Hannah Faye M. Austria[5], Tsung Han-Huang[5], Aditya Rianjanu[2,3], Canggih Setya Budi[4], Anawati Anawati[1], Wei-Song Hung[5*]

[1]*Department of Physics, Faculty of Mathematics and Natural Sciences, Universitas Indonesia, Depok, 16424, Indonesia*
[2]*Department of Materials Engineering, Institut Teknologi Sumatera, Jati Agung, Lampung Selatan, 35365, Indonesia*
[3]*Research Center for Green and Sustainable Materials, Institut Teknologi Sumatera, Jati Agung, Lampung Selatan, 35365, Indonesia*
[4]*Research Center for Polymer Technology, National Research and Innovation Agency (BRIN), The B.J. Habibie Science and Technology Area, South Tangerang, Banten, 15314, Indonesia*
[5]*Advanced Membrane Materials Research Center, Graduate Institute of Applied Science and Technology, National Taiwan University of Science and Technology, Taipei, 10607, Taiwan*
*__Corresponding author__: januar.widakdo@ui.ac.id, wshung@mail.ntust.edu.tw

Abstract
Organic solvent nanofiltration (OSN) is a promising separation technology with low energy consumption and environmental benefits. However, membrane stability in harsh organic solvents remains a challenge. Graphene oxide (GO) is widely explored due to its exceptional mechanical strength and selective permeability; however, further modifications are necessary to optimize its performance. This study investigates the enhancement of GO membranes by incorporating a thin-film composite (TFC) layer through interfacial polymerization using polyethyleneimine (PEI) and trimethyl chloride (TMC). The fabricated membranes were characterized for their morphology, chemical structure, and filtration performance using scanning electron microscopy (SEM), Fourier-transform infrared spectroscopy (FTIR), X-ray Photoelectron Spectroscopy (XPS), and contact angle measurements. Filtration tests were conducted with ethanol and Congo red dye solutions. The optimized membrane, composed of 0.1 wt% PEI 800 Mw and 0.05 wt% TMC, exhibited superior performance, demonstrating a permeance of 8.06 ± 2.31 L L m^{-2} h^{-1} bar^{-1} and a rejection rate of 95.20 ± 1.54% for Congo red dye. Additionally, the membrane exhibited a charge-dependent separation mechanism, achieving a 98.64 ± 0.38% rejection of methyl green due to both affinity and Donnan effects. These findings provide insights into developing advanced OSN membranes for efficient solvent purification and dye separation.

Keywords
Membrane, Organic Solvent Nanofiltration, Graphene Oxide, Thin-film Composite, Interfacial Polymerization

Received: 19 April 2025, Accepted: 6 July 2025
https://doi.org/10.26554/sti.2025.10.4.1031-1048

1. INTRODUCTION

Organic solvents are indispensable components in various industries, including pharmaceuticals, chemicals, food production, and materials engineering, where they serve as solvents for synthesis, extraction, and product formulation (Cseri et al., 2018; Naibaho et al., 2024; Rianjanu et al., 2025). Despite their extensive utility, improper management and disposal of organic solvents pose significant health and environmental hazards. They often contain toxic and volatile compounds, such as aromatic hydrocarbons (e.g., benzene and toluene) (Joshi and Adhikari, 2019), which can lead to severe environmental contamination and health issues ranging from minor irritations to chronic diseases (Saeedi et al., 2024). Additionally, the flammable nature of these solvents heightens the risk of industrial accidents, making efficient and sustainable handling and treatment strategies crucial (Cseri et al., 2018).

Organic solvent nanofiltration (OSN) has emerged as a transformative technology to address these challenges. By leveraging pressure-driven filtration, OSN enables the separation of small organic molecules from solvents without requiring energy-intensive phase changes (Gu et al., 2024), making it an environmentally friendly alternative to traditional methods such as distillation and adsorption (Gontarek-Castro and Castro-Muñoz, 2024). Furthermore, OSN offers modularity and scalability, which are critical for industrial applications (Xiao et al., 2024). However, the performance of OSN is often constrained by solvent-induced swelling, reduced separation efficiency, and structural instability of conventional membranes

(Wang et al., 2023).

Graphene oxide (GO) has gained significant attention as a next-generation material for membrane technology (Abdullah et al., 2024; Amri et al., 2023). Its unique two-dimensional structure, functionalized with oxygen-containing groups, provides exceptional mechanical strength (Liu et al., 2012; Pan et al., 2015; Widakdo et al., 2023), chemical resistance (Chen et al., 2012; Subrahmanya et al., 2022; Wan et al., 2012), and selective permeability (Thebo et al., 2018; Tian et al., 2022; Xu et al., 2015). GO membranes have demonstrated the ability to filter out dyes and other solutes while maintaining high solvent permeance (Huang et al., 2016). Nonetheless, the practical application of GO in OSN is hindered by challenges in achieving uniform layer deposition, controlling pore size, and minimizing defects that compromise performance (Austria et al., 2023; Nie et al., 2021). To overcome these limitations, thin-film composite (TFC) membranes have been explored as a solution. TFC membranes are characterized by a selective active layer fabricated via interfacial polymerization, which allows for precise control over layer thickness and chemical properties (Ji et al., 2021; Wen and Liu, 2022). This study introduces a novel approach to integrating GO with TFC membranes, leveraging the strengths of both materials to address their respective shortcomings. By combining the superior mechanical and chemical properties of GO with the tunability and durability of TFC layers, this research aims to develop a high-performance membrane for OSN applications.

The novelty of this research lies in the strategic use of interfacial polymerization to fabricate GO-TFC composite membranes, thereby optimizing the membrane's structural and functional properties. Previous studies have demonstrated the potential of TFC membranes in water treatment and reverse osmosis; however, their application in OSN, particularly with GO integration, remains underexplored (Grzebyk et al., 2022). Furthermore, this research investigates the effects of polyethyleneimine (PEI) and trimethyl chloride (TMC) concentrations on membrane performance, offering new insights into optimizing fabrication parameters for enhanced dye rejection and solvent permeance.

The expected benefits of this study extend beyond academic advancements. By improving the separation efficiency and stability of OSN membranes, the findings could reduce the environmental impact of industrial solvent use and enhance the sustainability of manufacturing processes. The developed membranes could also pave the way for broader applications in pharmaceutical purification, chemical synthesis, and wastewater treatment, contributing to a cleaner and more efficient industrial ecosystem. This study uniquely integrates GO nanosheets within a PEI/TMC-based TFC layer using low-molecular-weight PEI (800 Mw), achieving a superior balance of high permeance and selectivity for OSN applications, outperforming previous GO-based and conventional TFC membranes. In summary, this research addresses critical gaps in membrane technology by introducing and evaluating a novel GO-TFC composite membrane for OSN applications. The systematic exploration of material integration, fabrication techniques, and performance optimization underscores the innovative and practical significance of this work in advancing sustainable separation technologies.

2. EXPERIMENTAL SECTION

2.1 Materials

A few-layer graphene oxide suspension (2 wt%) was obtained from Angstron Materials Inc. (USA), while the supporting polyamide (N66) membrane (0.22 μm) was purchased from Hangzhou Anow Microfiltration Co., Ltd. (China). Amine functionalization was introduced by introducing polyethyleneimine (PEI, Mw ~800 Da) (Aldrich, USA) into the system. Benzene-1,3,5-tricarbonyl trichloride (TMC) (99.0%) was sourced from Sigma Aldrich. Various dyes, including methyl orange (MO), congo red (CR), methyl blue (MB), methyl green (MG), and disperse blue (DB), were also obtained from Sigma-Aldrich. Ethanol (95%, UNIWARD) was used without further purification. All chemicals in this study were utilized as received without further purification, and aqueous solutions were prepared using deionized water (≥18.2 mΩ -cm) (Uniss Super Pure Producer II, Taiwan).

2.2 Membrane Fabrication

The membrane fabrication process utilized a polyamide (PA) membrane substrate, specifically the Nylon 0.1 μm membrane, with dimensions of 310 mm and a thickness range of 0.11-0.12 mm. The fabrication procedure is schematically illustrated in Figure 1a. Initially, a thin layer of graphene oxide (GO) was deposited onto the PA substrate using a filter-assisted pressure technique at a pressure of 3 bars (Figure 1b). Subsequently, an interfacial polymerization process was employed to synthesize a thin-layer composite on the GO membrane surface. In this process, a dilute aqueous solution of polyethyleneimine in deionized water was poured onto the membrane and left for one minute. Afterward, the excess solution was removed. This step was followed by applying an organic solution of trimethyl chloride dissolved in *n*-hexane and poured for 30 seconds, with the excess solution similarly removed. The membrane was then subjected to heat treatment at 60°C for 10 minutes to enhance its physical strength and refine the pore structure.

2.3 Membrane Characterization

The membrane was thoroughly characterized to assess its structural, morphological, and surface properties. Attenuated Total Reflectance-Fourier Transform Infrared (ATR-FTIR) analysis was performed using a PerkinElmer Miracle-Dou model to determine the chemical composition and structure of the membrane's surface layer. The spectra were recorded in the wavenumber range of 650-4000 cm^{-1}. Scanning Electron Microscopy (SEM) was employed to examine the surface morphology and cross-sectional thickness of the membrane layers using a JEOL JSM-6900LV SEM. The images were subsequently processed with ImageJ software to evaluate pore structure and thickness. The hydrophilicity of the membrane sur-

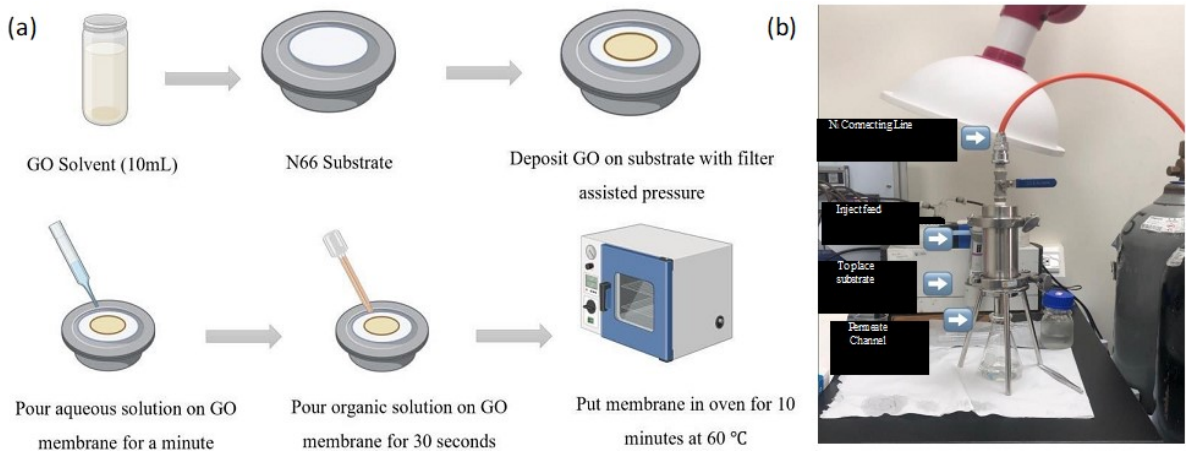

Figure 1. (a) Schematic of Membrane Fabrication, and (b) Set Instrument of Filter Assisted-Pressure

face was assessed through water contact angle measurements using DataPhysics OCA 25 software. Zeta potential analysis was conducted to characterize the surface charge of the membrane using an Anton Paar SurPASS 3 instrument, with measurements taken across a pH range of 3-11. X-ray Photoelectron Spectroscopy (XPS) (Model K-Alpha, Thermo Fisher, USA) was employed to analyze the functional groups present on the materials and to investigate their chemical compositions.

The research methodology began with the preparation of PA-based membranes. The membranes were tested for performance using an ethanol solution mixed with Congo red dye. This was followed by advanced characterization through UV-visible spectroscopy, ATR-FTIR, SEM, water contact angle measurement, and zeta potential analysis to validate the structural properties and performance of the fabricated membranes.

2.4 Membrane Performance Testing

The performance of the fabricated membranes was evaluated using the "Dead-End Filtration Process." The membranes were tested with an ethanol solution containing Congo red dye at a concentration of 20 ppm. Before testing, the membranes were compacted by circulating the ethanol solution for 30 to 60 minutes. This compaction step was crucial for determining the stabilization pressure for the performance tests. The filtration tests were conducted for 30 to 60 minutes at a stabilized pressure. Permeation flux (P) was calculated using the following equation.

$$P = \frac{V}{A \cdot t \cdot p}$$

where P represents the permeation flux (L m^{-2} h^{-1} bar^{-1}), V is the volume of permeate (L), A is the effective membrane area (m^2), t is the time (h), and p is the pressure (bar)

$$R(\%) = \left(1 - \frac{C_p}{C_f}\right) \times 100$$

C_p and C_f are the concentrations of the permeate and feed solutions, respectively.

3. RESULTS AND DISCUSSION

3.1 Morphology and Physical Characterization of Thin Film Composite Polymerization Membrane

The formation and characterization of thin composite membrane layers were systematically analyzed to evaluate their structural integrity and performance in nanofiltration processes. The digital photographs in Figures 2a-d show that visual inspection alone cannot distinguish between the nylon-66 substrate and the graphene oxide (GO) membrane, as the composite thin-film layer is highly transparent and extremely thin. Therefore, scanning electron microscopy (SEM) is essential for examining the surface morphology, structural changes, and thickness of the formed layers.

SEM analysis of the surface morphology (Figure 2 and Figures 4a-d) confirmed the successful formation of a thin composite film layer on the polyamide substrate. However, the layer formed on the nylon-66 substrate initially intended for ultrafiltration with a pore size of 0.1 μm proved unsuitable for nanofiltration. The SEM images revealed that the composite layer lacked adequate thickness and strong bonding with the substrate, making it prone to delamination or dissolution under high-pressure conditions. This highlights the necessity for additional structural enhancements to optimize the membrane's durability and filtration efficiency.

As demonstrated by SEM imaging, the addition of graphene oxide (GO) at a concentration of 1 ppm effectively reduced and closed the substrate's pores. Forming a uniform and defect-free thin-film composite (TFC) layer notably depended on the molecular weight of polyethyleneimine (PEI) used during fabrication. SEM images of GO membranes produced with different PEI molecular weights (800 Mw, 10,000 Mw, and 25,000 Mw) showed that the lower molecular weight PEI (800 Mw) facilitated the creation of a more uniform and defect-free composite thin-film layer. This observation aligns with pre-

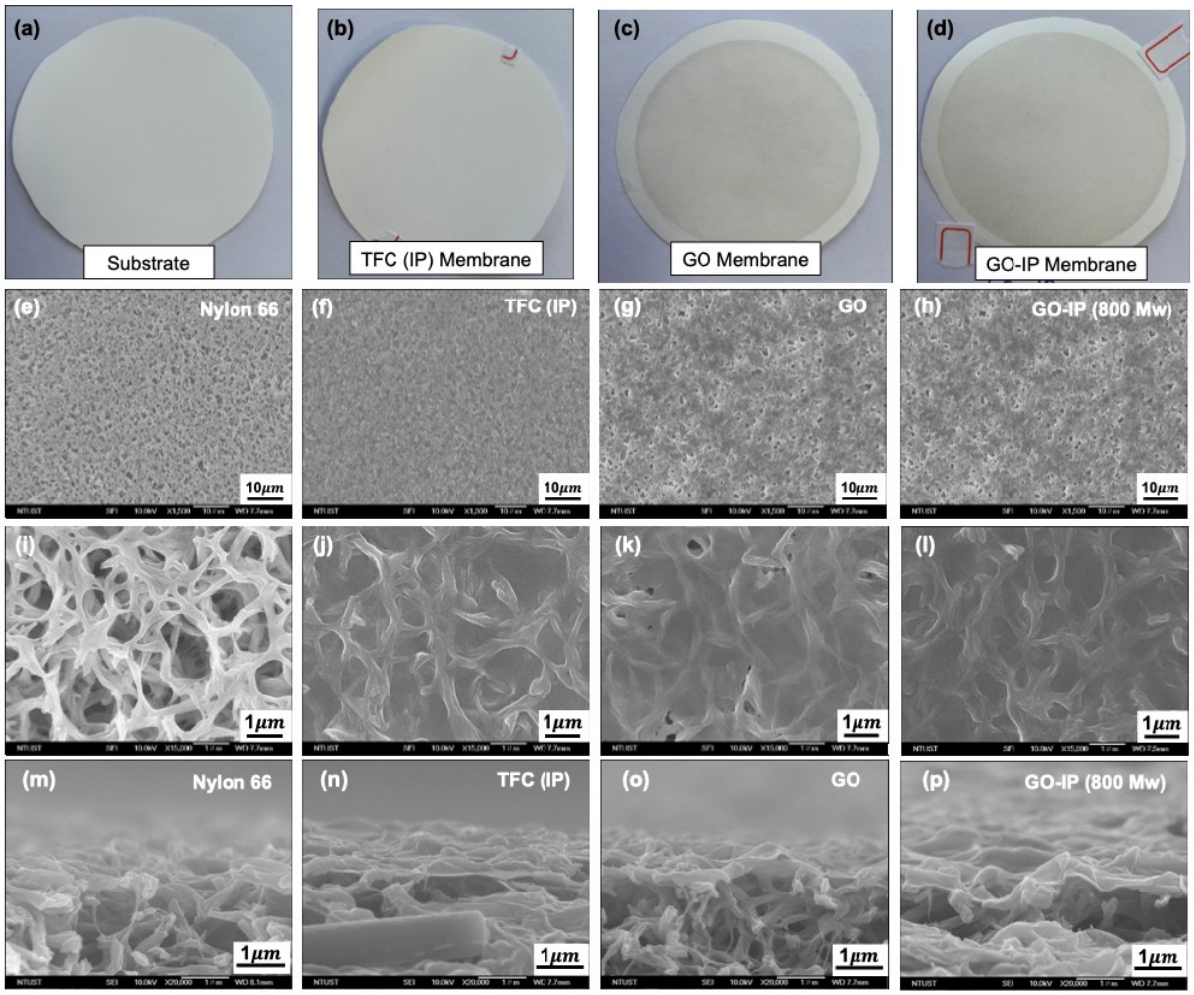

Figure 2. Photographic and SEM Characterization of Membrane Structures at Various Stages of Modification. Digital Photographs of Membranes: (a) Pristine Nylon-66 Substrate, (b) TFC Membrane Formed via Interfacial Polymerization (IP), (c) Graphene Oxide (GO) Coated Membrane, and (d) GO-TFC Composite (GO-IP, 800 Mw). SEM Surface Images at 1500× Magnification Showing Progressive Surface Morphology Changes from the Porous Substrate (e), to Smoother TFC (f), and More Compact Structures in GO (g) and GO-IP Membranes (h). Higher-Magnification Surface SEM Images (15,000×), Revealing the Porous Network of Nylon-66 (i), Smoother Polymer Coverage in TFC (j), Partially Covered Pores in GO (k), and More Uniform Coverage in GO-IP (l). (m–p) Cross-Sectional SEM Images Highlighting Structural Differences in Membrane Layers

vious reports suggesting that higher molecular weight PEI requires additional energy, catalysts, or processing time to achieve similar uniformity and defect-free characteristics.

The SEM cross-sectional analysis (Figures 2m-p) faced limitations in measuring the thickness of the composite thin-film layer due to its extreme thinness. Using only 1 ppm GO in a 10 mL solution resulted in a membrane layer that was difficult to observe in the cross-section and prone to combustion during SEM testing. These challenges underscore the need for advanced imaging techniques or alternative characterization methods to accurately evaluate the cross-sectional structure of ultrathin membrane layers.

Atomic force microscopy (AFM) further corroborated these findings, providing quantitative data on surface roughness (Ra) (Figures 3a-d and Figures 4e-f). The nylon-66 substrate exhibited the highest surface roughness, at 157 nm, which is attributable to its large pore size and uneven surface. Adding the TFC layer and GO modification substantially reduced surface roughness, with the GO-TFC membrane using PEI with a molecular weight of 800 achieving the lowest roughness value of 98.4 nm. As previously reported, this reduction in roughness enhances the membrane's structural integrity and optimizes its performance by mitigating flow resistance and increasing contact area with the solution (Joshi et al., 2015).

Despite the challenges related to characterizing ultrathin GO membranes, the results demonstrate the superior performance of the GO-TFC membrane made with PEI 800 Mw. The low surface roughness and uniform morphology highlight

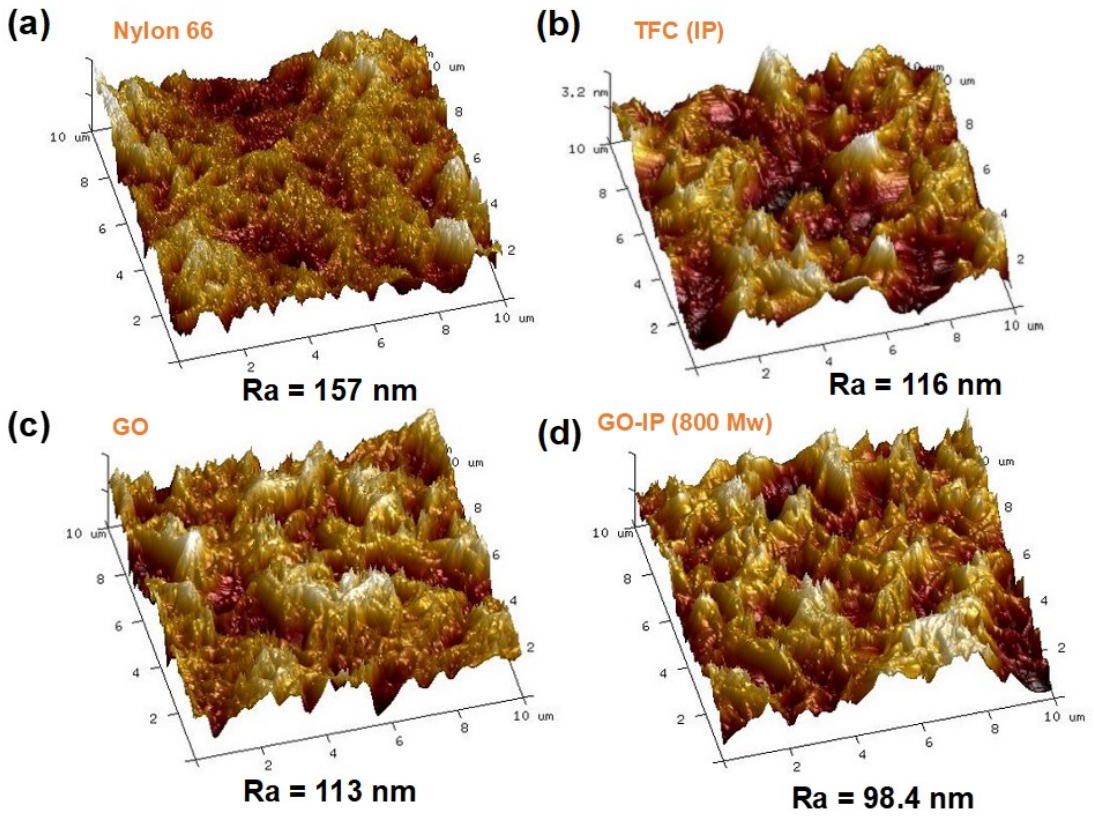

Figure 3. AFM Images of (a) Nylon-66, (b) TFC (IP) Membrane, (c) GO Membrane, (d) GO-IP (800 Mw) Membrane

its potential as a high-performance material for nanofiltration applications. However, the inability to achieve similar uniformity and defect-free characteristics with higher molecular weight PEI (10,000 Mw and 25,000 Mw) indicates that further optimization of fabrication parameters is necessary. This may involve exploring alternative cross-linking agents, catalysts, or longer reaction times to achieve the desired membrane properties. In summary, the study offers critical insights into the role of GO and PEI molecular weight in enhancing membrane morphology and performance. The findings establish a clear relationship between surface roughness, uniformity, and nanofiltration efficiency, thereby paving the way for the development of next-generation nanofiltration membranes tailored for specific applications.

3.2 Chemical Characterization of Thin Film Composite Polymerization Membrane

ATR-FTIR and water contact angle measurements characterized the surface chemical composition and hydrophilic properties of the membranes. These measurements offered insights into the functional groups present and their influence on membrane performance. The results highlight the essential role of graphene oxide (GO) and thin-film composite (TFC) layers in modifying and improving the membrane's properties.

The ATR-FTIR analysis (Figure 5a) revealed distinct peaks corresponding to the functional groups of the nylon-6.6 substrate, including hydroxyl (OH), carboxyl (C=O and C−O), aromatic (C=C), epoxy (C−O), and alkoxy (C−O) groups at wavenumbers of 3300, 1724, 1624, 1374, 1232, and 1064 cm^{-1}, respectively. The addition of GO introduced an increase in the intensity of the hydroxyl group peak at 3300 cm^{-1}, consistent with previous findings on the ATR-FTIR characteristics of GO membranes (Austria et al., 2023). This increase confirms the incorporation of GO into the membrane structure, as hydroxyl groups are a characteristic feature of GO. However, no new functional groups were observed with the addition of the composite thin film layer. This outcome can be attributed to two factors: (1) the thinness of the TFC layer, which limits its detectability via ATR-FTIR, and (2) the chemical similarity of functional groups between the nylon-6.6 substrate and the TFC membrane layer, both of which form a medium-long polyamide bond chain structure (Xie et al., 2021).

Figure 5b illustrates the repeating chain structure of the Nylon-66 substrate, which serves as the support layer for the thin-film membranes. Nylon-66 is synthesized via the polycondensation reaction between hexanedioic acid (adipic acid) and hexane-1,6-diamine, forming amide linkages (−C−NH−). These amide bonds contribute to the mechanical strength and chemical stability of the membrane, making it suitable for solvent-resistant applications (Farahani and Chung, 2018). Fig-

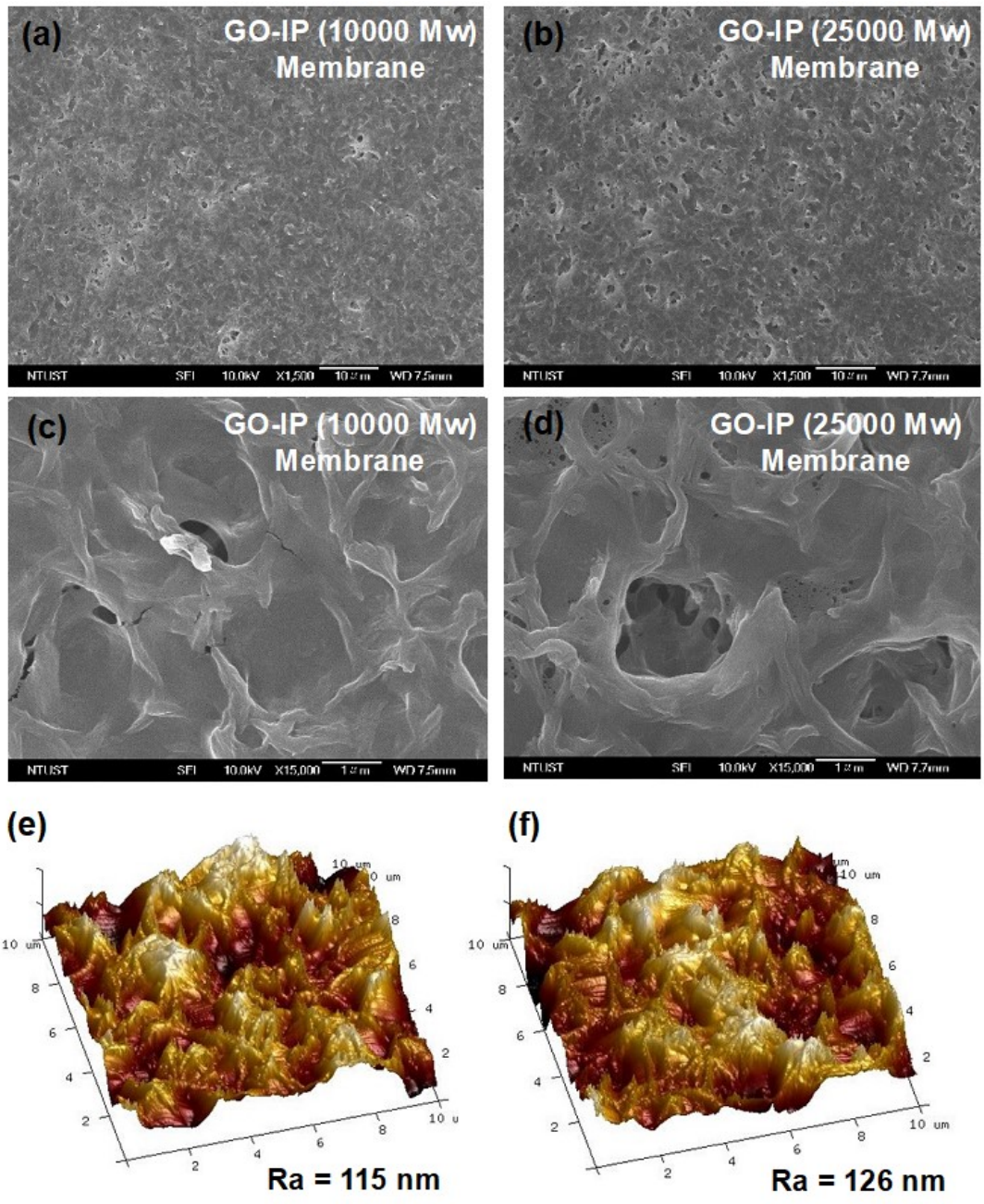

Figure 4. (Morphology of Membrane Surface Magnification 1500× (a) GO-IP (10,000Mw), (b) GO-IP (25,000Mw). Morphology of Membrane Surface Magnification 15,000× (c) GO-IP (10,000Mw), (d) GO-IP (25,000Mw). AFM Characterization Data of Membrane Surface (e) GO-IP (10,000Mw), (f) GO-IP (25,000Mw)

ure 5c depicts the interfacial polymerization reaction between polyethyleneimine (PEI) and Benzene-1,3,5-tricarbonyl trichloride (TMC). This reaction results in a crosslinked polyamide network that enhances membrane selectivity and durability. PEI, a branched polymer with multiple amine groups, reacts with the acyl chloride groups in TMC to form an ultrathin, dense, and selective separation layer. Reaction conditions, monomer concentrations, and variations in the molecular weight of incorporated GO can influence the degree of crosslinking and membrane performance (Qian et al., 2018).

Water contact angle measurements further demonstrated the effect of GO and TFC layers on the hydrophilic properties of the membranes (Figure 5d). The pristine nylon-6.6 substrate exhibited a water contact angle of 34.46 ± 6.07°, indicating hydrophilic characteristics suitable for supporting the formation of TFC layers (Marchetti et al., 2014). The

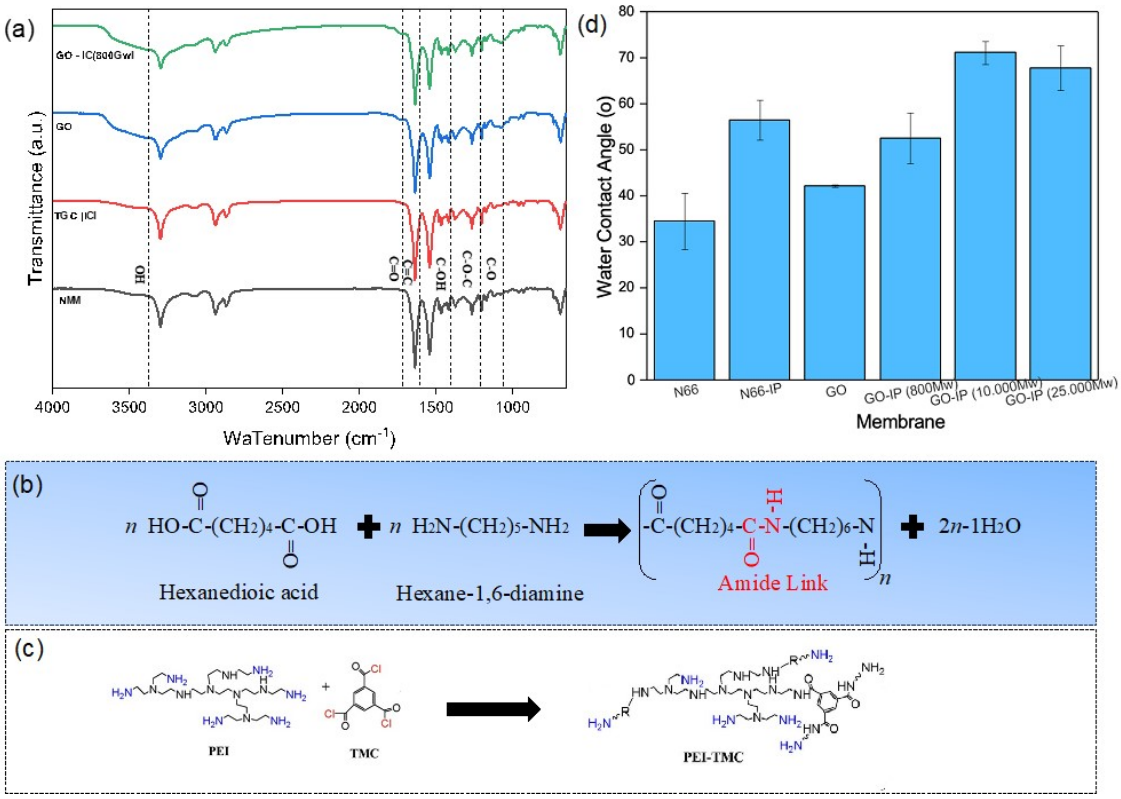

Figure 5. Chemical Structure Analysis and Hydrophilicity Characterization of Membrane Samples. (a) ATR-FTIR Spectra of the Nylon-66 Substrate, GO Membrane, TFC Membrane, and GO-IP (800 Mw) Membrane, Showing Characteristic Peaks Related to Hydroxyl, Amide, and Carboxyl Groups. The Spectra Confirm Successful Incorporation of GO and Polymer Layers, with Increased Peak Intensity Around 3300 cm^{-1} Indicating Enhanced –OH Functionality in GO and GO-IP Membranes. (b) Polymerization Reaction Forming the Repeating Amide Linkage in the Nylon-66 Substrate from Hexanedioic Acid and Hexane-1,6-Diamine, Highlighting the Formation of the –C–N– Bond Contributing to Membrane Stability. (c) Interfacial Polymerization Between Polyethyleneimine (PEI) and Trimesoyl Chloride (TMC), Resulting in a Crosslinked PEI-TMC Structure that Enhances the Membrane's Selective Layer. (d) Water Contact Angle Measurements for Various Membranes Showing Improved Hydrophilicity After GO and TFC Integration. GO-IP (800 Mw) Exhibits Optimal Surface Wettability, While Higher Molecular Weight PEI (10,000 and 25,000 Mw) Results in Less Hydrophilic Surfaces Due to Increased Roughness and Less Uniform Coating)

introduction of GO increased the contact angle to 42.16 ± 0.31°, reflecting its hydrophilic properties due to the hydroxyl groups forming hydrogen bonds with water molecules. This enhancement aligns with the known ability of GO to create a strong adhesion force with water, resulting in a well-distributed surface layer (Austria et al., 2023).

The TFC membrane exhibited a water contact angle of 56.52 ± 4.37°, indicating moderate hydrophilicity. Amine groups in the TFC layer contribute to its hydrophilic nature by forming hydrogen bonds with water molecules (Zhai et al., 2023). Incorporating GO into the TFC layer using polyethyleneimine (PEI) with a molecular weight of 800 Mw further enhanced the hydrophilic properties, as evidenced by a reduction in the water contact angle. This improvement can be attributed to the increased presence of hydroxyl groups from GO, which promote stronger interactions with water molecules.

Interestingly, membranes fabricated with higher molecular weight PEI (10,000 Mw and 25,000 Mw) did not exhibit a comparable increase in hydrophilic properties. SEM analysis suggests that these membranes have uneven and imperfect surface morphologies, which hinder the spreading of water across the surface. The irregularities and defects on the membrane surface can negatively impact the hydrophilic properties, even with the incorporation of GO. This finding highlights the importance of achieving a uniform, defect-free surface to optimize hydrophilic performance (Zhai et al., 2023).

Integrating GO and TFC layers into nylon-6.6 membranes significantly enhances their surface properties, especially hydrophilicity, which is crucial for membrane performance in filtration applications. The molecular weight of PEI used in the TFC fabrication process plays a key role in determining surface uniformity and hydrophilic characteristics. These find-

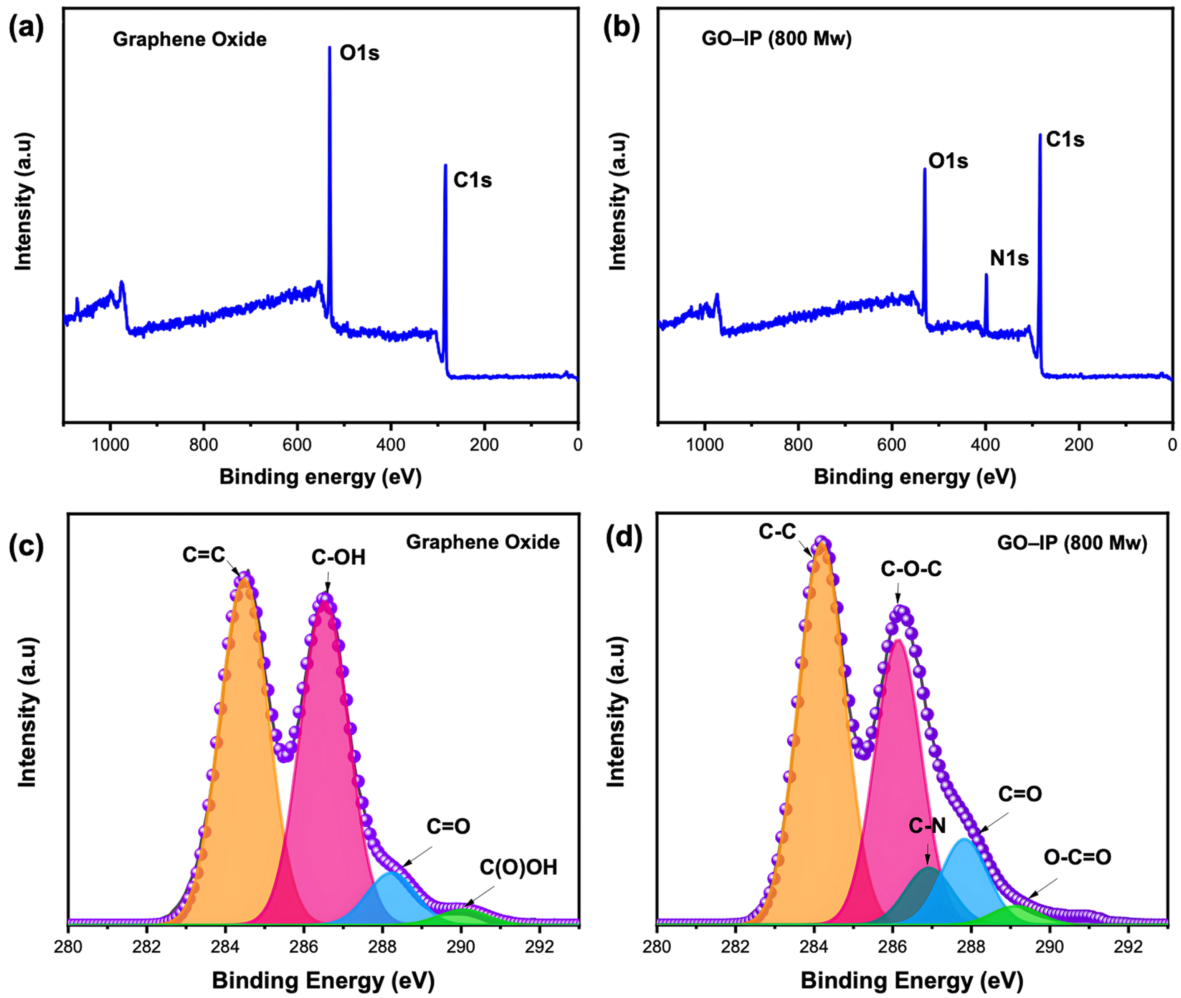

Figure 6. XPS Spectra of (a) GO and (b) GO-IP Membranes, (c) C1s XPS Spectrum of GO Membrane, (d) C1s XPS Spectrum of GO-IP (800 Mw) Membranes

ings offer valuable insights into designing high-performance membranes tailored for specific applications, highlighting the interaction between chemical composition, surface morphology, and functional performance.

The X-ray photoelectron spectroscopy (XPS) data presented in Figure 6 offer valuable insights into the surface chemistry of graphene oxide (GO) and graphene oxide-interfacial polymerization (GO-IP) membranes. The XPS spectra displayed in Figures 6a and 6b reveal the elemental composition of GO before and after interfacial polymerization. The GO membrane (Figure 6a) exhibits distinct peaks corresponding to oxygen (O1s) and carbon (C1s), confirming the presence of oxygen-containing functional groups, including hydroxyl, epoxy, and carboxyl groups. In contrast, the GO-IP membrane (Figure 6b) exhibits a decrease in oxygen-related peaks and the potential appearance of nitrogen (N1s) peaks, suggesting the successful incorporation of polymeric structures through interfacial polymerization.

The high-resolution C1s spectra presented in Figures 6c and 6d provide further insight into the chemical state of carbon in the membranes. The GO membrane (Figure 6c) exhibits peaks corresponding to C−C (sp^2 carbon from the graphene backbone), C−O (epoxy/hydroxyl), and O−C=O (carboxyl) functional groups, indicating its high oxidation state. Conversely, following interfacial polymerization, the GO-IP membrane (Figure 6d) shows changes in peak intensity, including a significant reduction in oxygen-functionalized carbon peaks and the emergence of a C−N peak. This indicates that the polymerization process altered the GO surface by forming new amide or amine bonds with the polymer matrix, resulting in a more crosslinked and chemically stable membrane structure (Widakdo et al., 2023). The decrease in oxygen functionalities and the formation of C−N bonds suggest that the interfacial polymerization process effectively enhanced the membrane properties, potentially improving its dye separation performance.

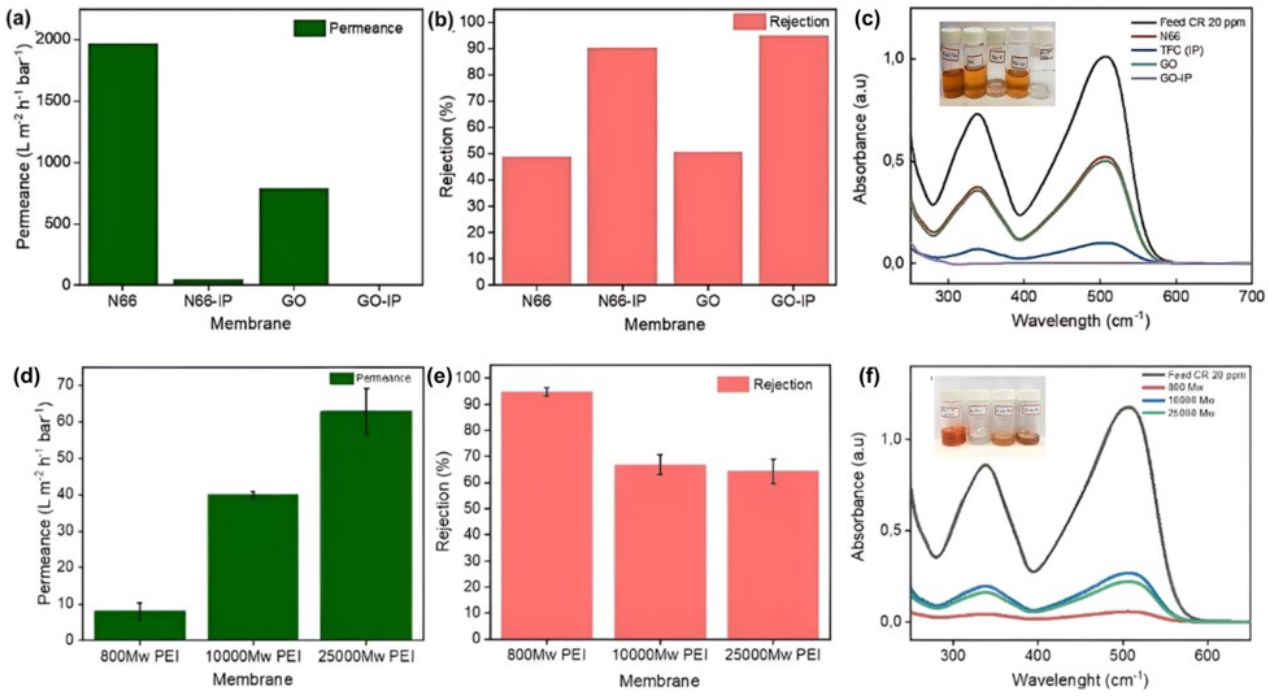

Figure 7. Performance of Membrane Nylon 66, TFC (IP), GO, GO-IP (a) Permeance, (b) Rejection, (c) UV-Vis Spectra of Performance. Performance GO-TFC (GO-IP) Membrane Mw Variation (d) Permeance, (e) Rejection, (f) UV-Vis Spectra of Performance

3.3 Dye Separation Performance

The performance evaluation of various membrane configurations, including nylon-66, thin-film composite (TFC) membranes, graphene oxide (GO), and GO-IP (Figures 7a-c), highlights the importance of structural modifications in enhancing filtration performance. The results indicate substantial variations in permeance and rejection rates, highlighting the necessity for advanced composite designs to achieve optimal outcomes.

The nylon-66 substrate, as a base ultrafiltration membrane, demonstrated exceptionally high permeance (1963.89 L m^{-2} h^{-1} bar^{-1}) but a low rejection rate (48.63%). These results align with its ultrafiltration characteristics, allowing the solvent and solute (dissolved dyes) to pass through with minimal resistance (Chang et al., 2021). This trade-off between high permeance and poor solute rejection emphasizes the need for surface modifications to enhance selective filtration.

Incorporating a GO layer onto the nylon-66 substrate resulted in a GO membrane with a reduced permeance of 785.56 L m^{-2} h^{-1} bar^{-1} and a slightly improved rejection rate of 50.53%. The modest enhancement in rejection can be attributed to the introduction of the GO layer, which adds a degree of size exclusion and adsorption capability to the membrane. However, the relatively small concentration of GO (1 ppm in a 10 mL solution) was insufficient to form a robust and continuous layer that could significantly improve performance. Prior studies have demonstrated that higher GO concentrations, such as 10 ppm, yield more substantial improvements in water purification applications (Austria et al., 2023). This indicates that optimizing the GO concentration is essential for maximizing the functional benefits of GO-modified membranes.

Creating a TFC layer using interfacial polymerization (IP) on the nylon-66 substrate significantly enhanced membrane performance. The TFC membrane achieved a rejection rate of 90.05%, with a permeance of 48.70 L m^{-2} h^{-1} bar^{-1}. This improvement can be attributed to the TFC layer's ability to filter out dissolved particles while maintaining reasonable water flux selectively. However, these results were inconsistent with those reported in prior studies, where similar TFC membranes demonstrated superior performance metrics (Cheng et al., 2021; Zhai et al., 2023; Zhao et al., 2022). This discrepancy may arise from variations in synthesis parameters, including monomer concentration, polymerization time, and post-treatment conditions, which require further investigation.

The TFC and GO membranes were combined into a hybrid configuration to address these limitations and achieve improved performance. The synergistic effect of the GO and TFC layers is anticipated to enhance both rejection and permeance by utilizing the hydrophilic and adsorptive properties of GO along with the size exclusion and selective filtration capabilities of the TFC layer. Integrating these complementary mechanisms represents a promising strategy for overcoming the limitations of individual membrane configurations, paving the way for more effective filtration solutions.

The progressive modifications from nylon-66 to GO and

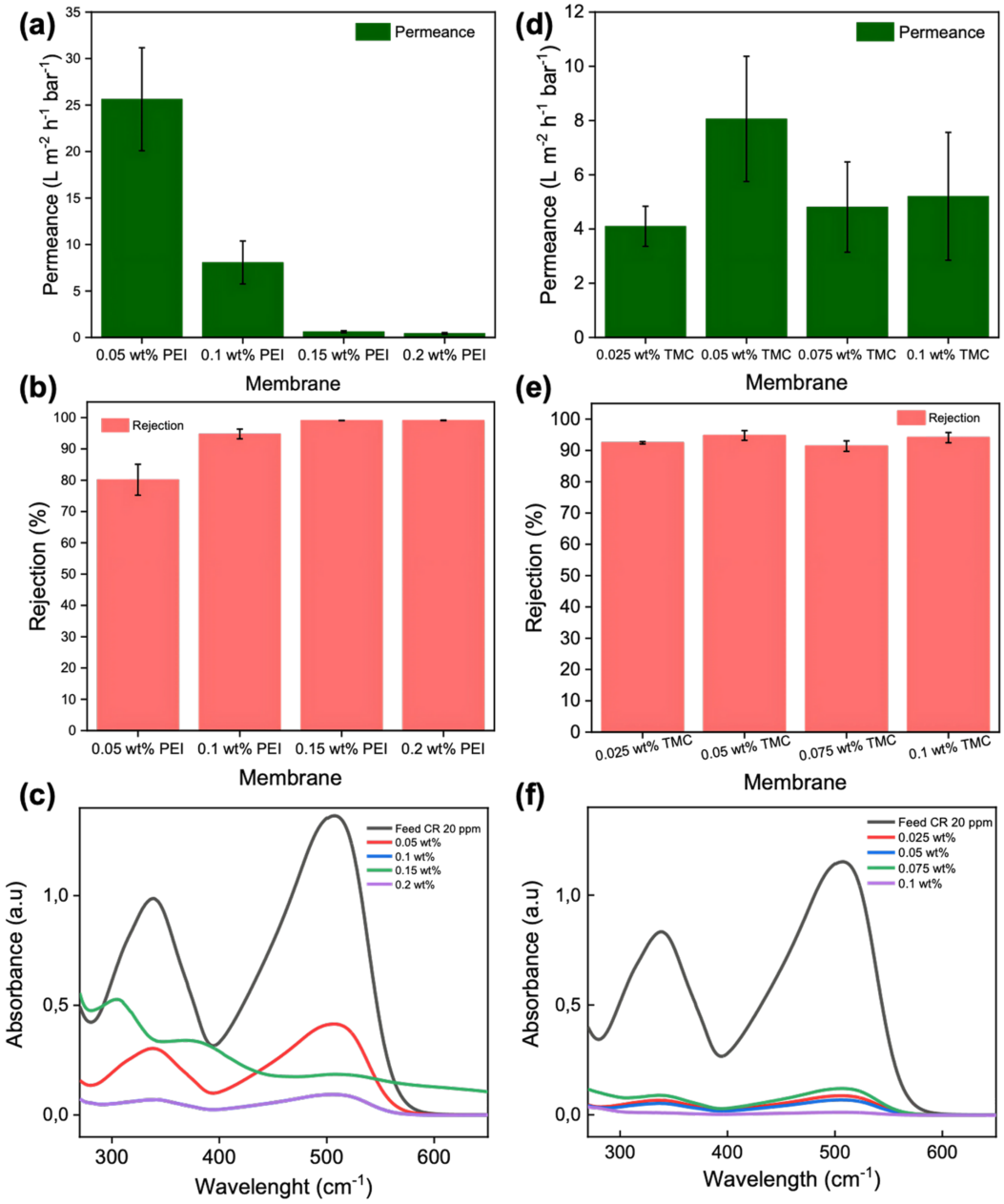

Figure 8. Performance of Membrane Nylon 66, TFC (IP), GO, GO-IP (a) Permeance, (b) Rejection, (c) UV-Vis Spectra of Performance. Performance GO-TFC (GO-IP) Membrane Mw Variation (d) Permeance, (e) Rejection, (f) UV-Vis Spectra of Performance

TFC membranes highlight the potential of composite designs to enhance filtration performance. The findings underscore the importance of optimizing material composition and synthesis processes to achieve high rejection rates while maintaining permeance. Future research should aim to fine-tune the integration of GO and TFC layers, explore higher GO concentrations, and investigate the impact of interfacial polymerization parameters to improve the performance of hybrid membranes further.

The performance analysis of composite thin-film membranes enhanced with graphene oxide (GO) and polyethyleneimine (PEI) of different molecular weights offers critical insights into the relationship between membrane structure, material properties, and filtration efficiency (Figures 7d-f). The

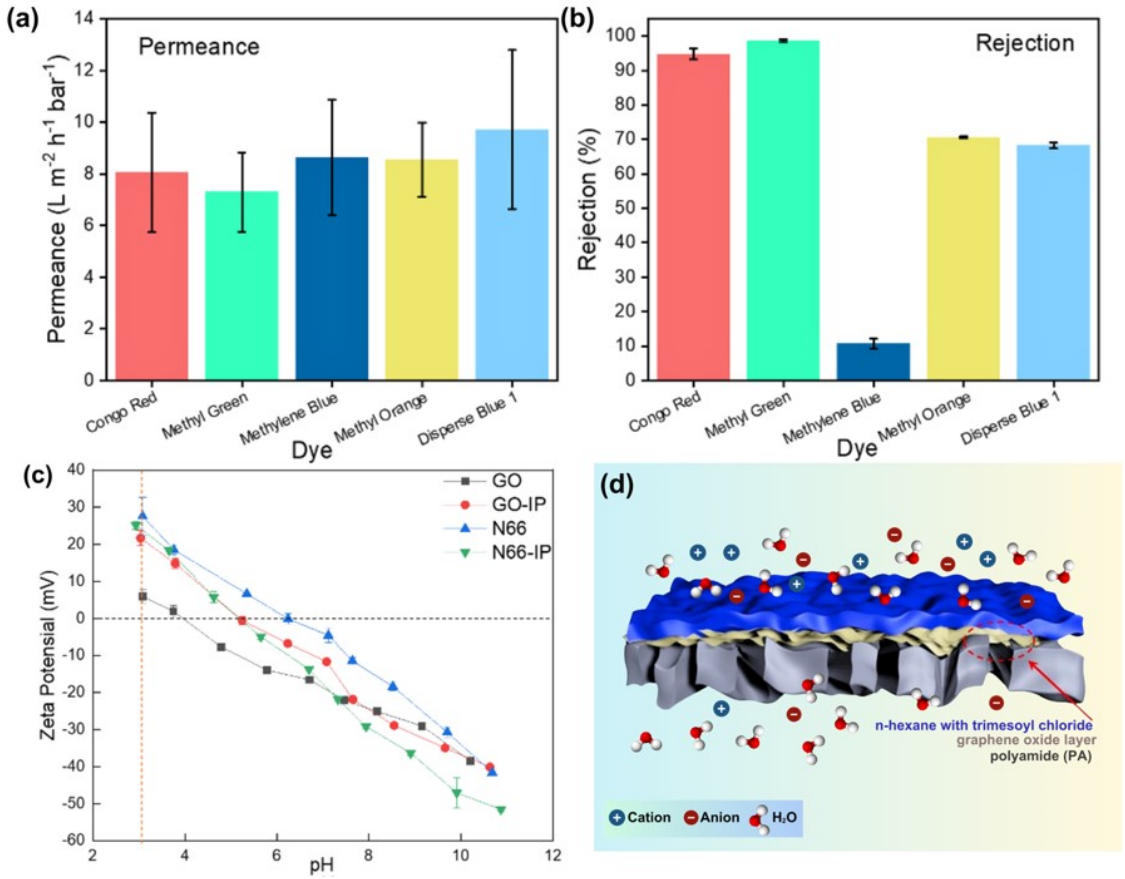

Figure 9. Performance GO-TFC (GO-IP) Membrane in Different Dyes (a) Permeance, (b) Rejection, (c) Zeta Potential Characteristics, and (d) Graphical Abstract for the Dye Separation Process

results emphasize the importance of choosing suitable molecular weights and optimizing synthesis parameters to achieve high rejection rates and acceptable permeance.

The study revealed that membranes fabricated with PEI 800 Mw exhibited the most favorable performance, achieving the highest rejection rate of 95.20 ± 1.54% with a permeance of 8.06 ± 2.31 L m^{-2} h^{-1} bar^{-1} (See Figures 7d-f). These findings are consistent with the theory that lower permeance generally correlates with higher rejection, as the dense and uniform surface structure limits solute passage (Zhao et al., 2022). Scanning electron microscopy (SEM) confirmed the structural integrity of these membranes, demonstrating the formation of a defect-free and uniform composite layer. This uniformity plays a critical role in enhancing rejection by ensuring that no solution bypasses the filtration barrier through imperfections.

In contrast, membranes incorporating PEI with molecular weights of 10,000 Mw and 25,000 Mw exhibited higher permeances of 39.94 ± 0.88 and 62.84 ± 6.63 L m^{-2} h^{-1} bar^{-1}, respectively, but significantly lower rejection rates of 66.88 ± 4.65% and 64.40 ± 3.67%. The increased permeance and lower rejection rates can be attributed to structural defects observed in SEM images. These membranes displayed non-uniform surfaces with defects such as shafts and larger pores, which likely allowed the solution, including dye particles, to pass through unfiltered. Moreover, these defects can cause the membrane to collapse under high-pressure conditions, exacerbating performance issues. These observations underscore the trade-offs associated with using higher molecular weight PEI, where the increased viscosity during the interfacial polymerization process can hinder the formation of a smooth and uniform thin-film layer.

Subsequent optimization efforts focused on TFC and GO membranes fabricated using PEI 800 Mw at varying concentrations. By systematically adjusting the PEI concentration from 0.05 wt% to 0.2 wt% while maintaining a constant TMC concentration of 0.05 wt%, the study aimed to refine the balance between permeance and rejection. The selection of PEI 800 Mw for this optimization was based on its superior performance in previous tests compared to other molecular weights. Such efforts align with the existing literature, which emphasizes the significance of polymer concentration in controlling the thickness, density, and overall performance of TFC membranes (Cheng et al., 2021).

The findings suggest that the molecular weight of PEI is

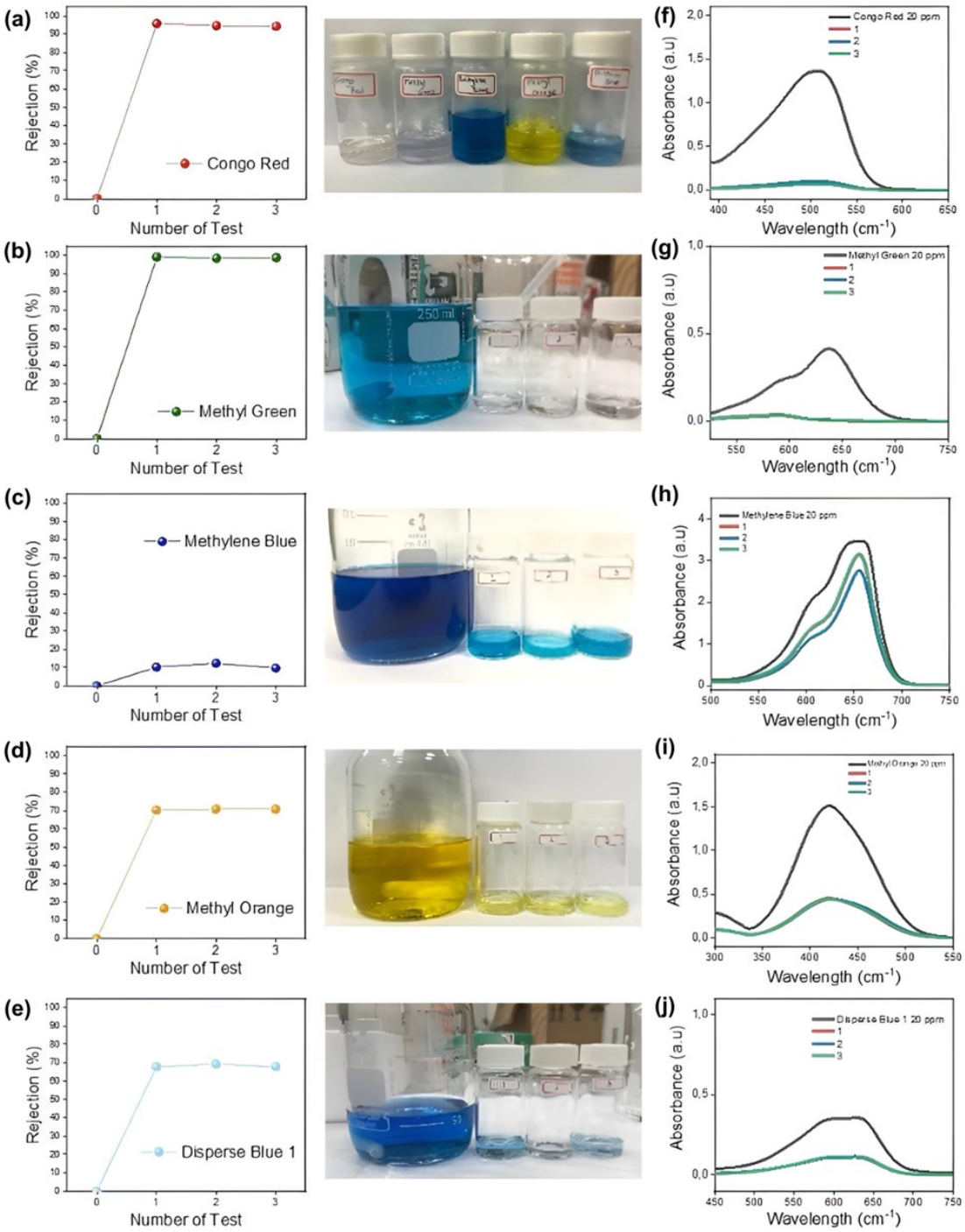

Figure 10. Number of Test Performance Dyes (a-e), (f-j) UV-visible Spectra of Dyes Congo Red, Methyl Green, Methylene Blue, Methyl Orange, Disperse Blue 1

a crucial factor in determining membrane performance, as it affects the structural characteristics and filtration properties of the composite layer. The membranes made with PEI 800 Mw exhibit superior performance due to their capacity to form a defect-free, dense, and uniform layer that effectively balances high rejection rates with reasonable permeance. In contrast, higher molecular weights lead to non-uniform membrane structures with significant defects, resulting in suboptimal filtration performance.

The performance evaluation of graphene oxide-based thin-film composite (GO-TFC) membranes synthesized via interfacial polymerization (GO-IP) with varying polyethyleneimine

Table 1

Dye	Molar weight (Da)	Charge	Molecular structure	pH	References
Methyl orange (MO)	327.33	Negative	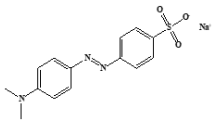	3	(Wu et al., 2021)
Congo red (CR)	696.67	Negative	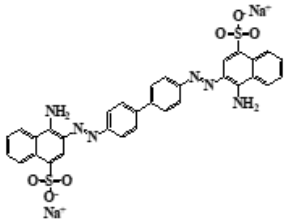	3 - 5.2	(Swan and Zaini, 2019)
Methyl blue (MB)	319.85	Positive	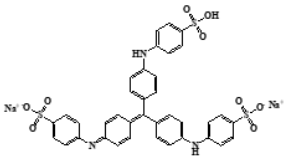	2 - 3.5	(Barton, 1987)
Methyl green (MG)	653.24	Positive	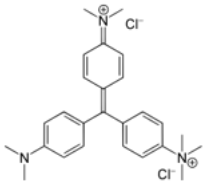	2 – 3.5	(Abegunde et al., 2024)
Disperse blue 1 (DB)	268.27	Neutral	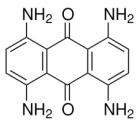	3	(Oguzie et al., 2021)

(PEI, 800 Mw) and Benzene-1,3,5-tricarbonyl trichloride (TMC) concentrations provides critical insights into their separation efficiency in organic solvent nanofiltration (OSN) applications. Figures 8a and 8d demonstrate that membrane permeance is highly dependent on the monomer concentration, exhibiting a decreasing trend with increasing PEI content due to enhanced crosslinking, which reduces free volume and restricts solvent transport. However, TMC concentration exhibits an optimal point where excessive polymer deposition causes additional transport resistance, leading to diminished flux. Comparatively, previous studies have reported similar trends, such as those noted by Wang et al. (2022) reported that excessive monomer deposition in polyamide (PA) membranes resulted in higher mass transfer resistance and reduced solvent permeation.

Figures 8b and 8e illustrate that rejection performance improves with increased monomer concentration, which aligns with previous findings (Wei et al., 2011), where the densification of the selective layer enhances the molecular sieving effect. Notably, our GO-TFC membranes exhibit superior rejection (> 98%) while maintaining higher permeance (>7 L m^{-2} h^{-1} bar^{-1}) compared to conventional interfacially polymerized PA membranes, which generally achieve permeance values around 2-5 L m^{-2} h^{-1} bar^{-1} under similar conditions. The UV-Vis spectra in Figures 8c and 8f further support the rejection performance, showing a significant reduction in dye concentration in the permeate stream, indicating improved selective layer integrity.

When benchmarked against other OSN membranes, our GO-TFC membranes exhibit a more favorable balance between permeability and selectivity compared to conventional PA/crosslinked Matrimid PI membranes (Hermans et al., 2015) and PDA/P84 PI membranes (Xu et al., 2017), which suffer from lower permeance (0.9–2.7 L m^{-2} h^{-1} bar^{-1}) at comparable rejection rates. Polymeric membranes fabricated via coating methods, such as PTSMP/PAN and PIM-1/cellophane (Shen et al., 2017; Volkov et al., 2009), often exhibit high permeance but lower selectivity, or vice versa, which limits their practical applicability in OSN. The incorporation of GO in the selective layer is essential for enhancing membrane performance, as it introduces additional transport pathways while maintaining structural integrity. This work illustrates that fine-tuning interfacial polymerization conditions can significantly improve membrane performance, making GO-TFC membranes a promising candidate for next-generation OSN applications.

The performance of GO-TFC (GO-IP) membranes for

Table 2. Comparison of the Performance with Other Works

TFC Types	Membrane Materials (Substrate/Surface selectivity)	Permeance (L m^{-2} h^{-1} bar^{-1})	Selectivity (%)	References
Interfacial Polymerization	PA/crosslinked Matrimid PI	2.7 (ethanol)	100 (1017 $g.mol^{-1}$)	(Hermans et al., 2015)
Interfacial Polymerization	PDA/crosslinked P84PI	0.9 (ethanol)	60 (327 $g.mol^{-1}$)	(Xu et al., 2017)
Coating	PTSMP/PAN	4.8 (ethanol)	90 (626 $g.mol^{-1}$)	(Volkov et al., 2009)
Coating	PIM-1/cellophane	0.06 (ethanol)	98 (626 $g.mol^{-1}$)	(Shen et al., 2017)
Interfacial Polymerization	GO/crosslinked PEI 800Mw	8.06 ± 2.31 (ethanol)	95.20 ± 1.54 (697 $g.mol^{-1}$)	This Work
Interfacial Polymerization	GO/crosslinked PEI 800Mw	7.30 ± 1.54 (ethanol)	98.64 ± 0.38 (653.24 $g.mol^{-1}$)	This Work

dye separation was evaluated by measuring permeance and rejection across different dye molecules, as illustrated in Figures 9(a) and 9(b). The permeance values varied slightly for different dyes, ranging from approximately 6 to 10 L m^{-2} h^{-1} bar^{-1}, demonstrating that the membrane maintains stable solvent transport properties despite variations in dye structure and molecular weight. Table 1 provides key characteristics of the key characteristics, including their molecular weight, charge, and pH conditions, which are critical factors influencing membrane performance. For instance, Congo Red (696.67 Da) and Methyl Green (653.24 Da), both large molecules, exhibited nearly 100% rejection due to their size exclusion and charge interactions. Conversely, Methylene Blue, with a smaller molecular weight of 319.85 Da and a positive charge, demonstrated the lowest rejection rate, indicating that charge interactions and molecular size influence separation efficiency. These results align with previous studies (Kang et al., 2020; Yang et al., 2023), which have demonstrated that interfacial polymerization-based membranes exhibit higher rejection rates for negatively charged and larger molecular weight dyes due to electrostatic repulsion and steric hindrance effects.

Figure 9c presents the zeta potential analysis, showing a declining trend in surface charge with increasing pH for different membrane types. The GO-TFC membrane exhibits a negative charge across a wide pH range, enhancing the rejection of negatively charged dyes such as Methyl Orange and Congo Red, which are strongly repelled due to electrostatic interactions, as shown in Table 1. This observation is consistent with prior research on graphene oxide-based membranes. Compared to conventional polymeric membranes, such as N66 and N66-IP, the GO-IP membrane exhibits improved charge stability, which contributes to its superior antifouling properties and long-term performance in dye filtration applications.

Lastly, Figure 9d provides a graphical abstract illustrating the mechanism of dye separation in the GO-TFC membrane, where the polyamide selective layer reinforced with graphene oxide forms a highly selective barrier for dye molecules while allowing the passage of solvents. *n*-hexane and trimesoyl chloride used in the polymerization process ensure a dense yet permeable selective layer with enhanced dye-rejection capabilities. As indicated in Table 1, the charge characteristics of the dyes are crucial to their separation behavior, with positively charged dyes such as Methyl Green and Methylene Blue being less effectively rejected than negatively charged dyes. Compared to conventional polymeric membranes, integrating graphene oxide introduces additional water transport pathways while maintaining excellent selectivity, making these membranes highly promising for efficient dye removal applications in wastewater treatment.

Figure 10 shows the dye rejection performance of the fabricated membrane across multiple test cycles, along with the corresponding UV-visible absorbance spectra for various dyes. The rejection efficiency for Congo Red, Methyl Green, Methylene Blue, Methyl Orange, and Disperse Blue 1 (Figures 10a-e) exhibits a rapid increase to nearly 100% after the first test cycle, indicating the membrane's high selectivity and separation capability. In contrast, Methylene Blue (Figure 10c) displays lower rejection, possibly due to its smaller molecular size or weaker interaction with the membrane surface.

The UV-visible spectra (Figures 10f-j) further confirm the dye rejection performance. The initial dye solutions exhibit distinct absorption peaks corresponding to their respective chromophores, but the absorbance intensity is significantly reduced after membrane filtration. This decrease in peak intensity after multiple test cycles suggests that the membrane effectively removes dye molecules from the solvent phase, thereby improving solvent purity. The results indicate that incorporating graphene oxide into the TFC membrane enhances its separation performance, likely due to improved hydrophilicity, structural stability, and selective interaction with dye molecules. These findings align with previous studies on graphene oxide-modified membranes, demonstrating enhanced dye removal efficiency through size exclusion, electrostatic interactions, and π–π stacking mechanisms (Nawi et al., 2024). The high rejec-

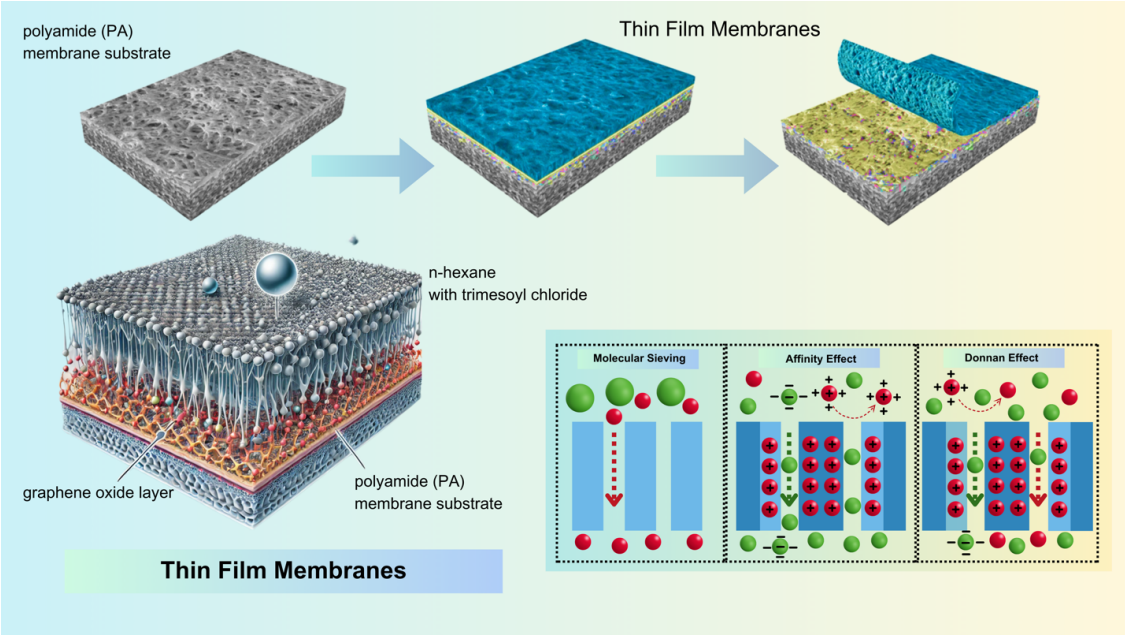

Figure 11. Schematic Diagram of the Polyamide (PA) Membrane Substrate and the Thin Layer Formed via Interfacial Polymerization on the Graphene Oxide (GO) Membrane Surface for Dye Separation in Organic Solvents

tion rates and considerable absorbance reduction underscore the membrane's potential for efficient dye separation in organic solvent applications. This makes it a promising candidate for wastewater treatment and industrial dye recovery processes.

Figure 11 presents a schematic depiction of the fabrication and functioning mechanism of thin-film composite (TFC) membranes integrated with graphene oxide (GO) for dye separation in organic solvents. The illustration emphasizes the interfacial polymerization process, in which a polyamide (PA) layer is formed on a porous PA membrane substrate. Graphene oxide within the membrane structure enhances its separation performance by introducing nanoscale structural modifications and functional groups that improve hydrophilicity, mechanical stability, and selective transport characteristics. The figure illustrates the molecular-level interactions that contribute to the membrane's high separation efficiency. The bottom-left section illustrates the GO layer within the membrane structure, which facilitates the rejection of dye molecules through size exclusion, electrostatic interactions, and affinity effects. During interfacial polymerization, trimethyl chloride in an organic solvent (*n*-hexane) reacts with an aqueous amine solution to create a thin, selective polyamide layer, further improving the membrane's performance in organic solvent filtration.

On the right side of the figure, three key separation mechanisms are highlighted: molecular sieving, the affinity effect, and the Donnan effect. Molecular sieving occurs when dye molecules are selectively rejected based on size, allowing only smaller molecules to pass through the membrane pores. The affinity effect utilizes electrostatic and chemical interactions between the dye molecules and the charged functional groups within the membrane, enabling selective separation based on charge properties. Finally, the Donnan effect describes the role of charged species in controlling ion transport across the membrane, which further contributes to enhanced dye rejection. This schematic effectively illustrates the role of graphene oxide-enhanced TFC membranes in organic solvent nanofiltration, demonstrating their potential for highly efficient dye removal. These findings align with previous research highlighting the benefits of GO-incorporated membranes for solvent-resistant separations, where enhanced selectivity and durability are crucial for industrial applications.

The comparison of TFC membranes in this study against previous works demonstrates significant improvements in permeance and selectivity for ethanol-based separations (Table 2). Among earlier interfacial polymerization-based membranes, PA/crosslinked Matrimid PI exhibited permeance of 2.7 L m^{-2} h^{-1} bar^{-1} with 100% selectivity for 1017 g·mol^{-1} molecules (Hermans et al., 2015), while PDA/crosslinked P84PI showed lower permeance (0.9 L m^{-2} h^{-1} bar^{-1}) and selectivity (60% for 327 g·mol^{-1}) (Xu et al., 2017). Coating-based membranes such as PTSMP/PAN achieved higher permeance (4.8 L m^{-2} h^{-1} bar^{-1}) with 90% selectivity for 626 g·mol^{-1} molecules, whereas PIM-1/cellophane displayed minimal permeance (0.06 L m^{-2} h^{-1} bar^{-1}) but high selectivity (98%) (Shen et al., 2017; Volkov et al., 2009). In contrast, the GO/crosslinked PEI 800 Mw membranes developed in this study significantly outperformed previous membranes, achieving permeances of 8.06 ± 2.31 and 7.30 ± 1.54 L m^{-2} h^{-1} bar^{-1} with selectivities of 95.20 ± 1.54% (697 g·mol^{-1}) and 98.64 ± 0.38% (653.24 g·mol^{-1}), respectively. These enhancements underscore the

effectiveness of incorporating GO and PEI into the polyamide thin-film layer, thereby improving hydrophilicity and molecular selectivity, and making them promising candidates for efficient organic solvent nanofiltration applications.

4. CONCLUSIONS

The integration of a graphene oxide (GO) layer (1 ppm) with a thin-film composite (TFC) membrane fabricated using 0.1 wt% PEI (800 Mw) and 0.05 wt% TMC significantly enhances membrane performance compared to using either component alone. The resulting GO-TFC membrane exhibited a uniform, hydrophilic surface with tunable surface charge and demonstrated excellent separation performance, achieving a permeance of 8.06 ± 2.31 L m^{-2} h^{-1} bar^{-1} and a 95.20 ± 1.54% rejection for Congo red. Notably, the membrane achieved 98.64 ± 0.38% rejection for methyl green, attributed to both molecular size exclusion and charge-based interactions. These findings underscore the importance of precise control over monomer type and concentration in optimizing membrane structure and function. For future research, long-term stability assessments under continuous operation and evaluation in real-world organic solvent nanofiltration (OSN) scenarios are recommended to validate scalability and industrial applicability.

5. ACKNOWLEDGEMENT

The authors sincerely thank the National Science and Technology Council (NSTC), Taiwan, for financially supporting this research (NSTC 113-2923-E-001-003-MY3). Also, this work was supported by Hibah Riset FMIPA UI Tahun Anggaran 2023-2024.

REFERENCES

Abdullah, H. W., T. H. Mubarak, and K. K. Resan (2024). A Graphene Oxide Nano-Sheets: A Novel Eco-Friendly Approach for Tissue Engineering and Antibacterial Applications in Bone Disease. *Science and Technology Indonesia*, **9**(4); 806–817

Abegunde, S. M., M. A. Adebayo, and E. F. Olasehinde (2024). Green Synthesis of ZnO Nanoparticles and Its Application for Methyl Green Dye Adsorption. *Green Energy and Resources*, **2**(2); 100073

Amri, A., A. Lesbani, and R. Mohadi (2023). Malachite Green Dye Adsorption From Aqueous Solution Using a Ni/Al Layered Double Hydroxide-Graphene Oxide Composite Material. *Science and Technology Indonesia*, **8**(2); 280–287

Austria, H. F. M., J. Widakdo, O. Setiawan, T. Subrahmanya, W.-S. Hung, C.-F. Wang, C.-C. Hu, K.-R. Lee, and J.-Y. Lai (2023). Tailoring the Specific Crosslinking Sites of Graphene Oxide Framework Nanosheets for Controlled Nanofiltration of Salts and Dyes. *Journal of Cleaner Production*, **395**; 136280

Barton, S. S. (1987). The Adsorption of Methylene Blue by Active Carbon. *Carbon*, **25**(3); 343–350

Chang, C.-M., H.-T. Chen, S.-H. Chuang, H.-C. Tsai, W.-S. Hung, and J.-Y. Lai (2021). Mechanisms of One-Dimensional and Two-Dimensional Synergistic Thermal Responses on Graphene Oxide-Modified PNIPAm Framework Membranes for Control of Molecular Separation. *Separation and Purification Technology*, **266**; 118568

Chen, D., H. Feng, and J. Li (2012). Graphene Oxide: Preparation, Functionalization, and Electrochemical Applications. *Chemical Reviews*, **112**(11); 6027–6053

Cheng, X., Y. Qin, Y. Ye, X. Chen, K. Wang, Y. Zhang, A. Figoli, and E. Drioli (2021). Finely Tailored Pore Structure of Polyamide Nanofiltration Membranes for Highly-Efficient Application in Water Treatment. *Chemical Engineering Journal*, **417**; 127976

Cseri, L., M. Razali, P. Pogany, and G. Szekely (2018). Organic Solvents in Sustainable Synthesis and Engineering. In *Green Chemistry*. Elsevier, pages 513–553

Farahani, M. H. D. A. and T.-S. Chung (2018). Solvent Resistant Hollow Fiber Membranes Comprising P84 Polyimide and Amine-Functionalized Carbon Nanotubes with Potential Applications in Pharmaceutical, Food, and Petrochemical Industries. *Chemical Engineering Journal*, **345**; 174–185

Gontarek-Castro, E. and R. Castro-Muñoz (2024). How to Make Membrane Distillation Greener: A Review of Environmentally Friendly and Sustainable Aspects. *Green Chemistry*, **26**(1); 164–185

Grzebyk, K., M. D. Armstrong, and O. Coronell (2022). Accessing Greater Thickness and New Morphology Features in Polyamide Active Layers of Thin-Film Composite Membranes by Reducing Restrictions in Amine Monomer Supply. *Journal of Membrane Science*, **644**; 120112

Gu, S., S. Li, and Z. Xu (2024). Organic Solvent Nanofiltration Membranes for Separation in Non-Polar Solvent System. *Green Energy & Environment*, **10**(2); 244–267

Hermans, S., E. Dom, H. Mariën, G. Koeckelberghs, and I. F. Vankelecom (2015). Efficient Synthesis of Interfacially Polymerized Membranes for Solvent Resistant Nanofiltration. *Journal of Membrane Science*, **476**; 356–363

Huang, L., J. Chen, T. Gao, M. Zhang, Y. Li, L. Dai, L. Qu, and G. Shi (2016). Reduced Graphene Oxide Membranes for Ultrafast Organic Solvent Nanofiltration. *Adv. Mater*, **28**(39); 8669–8674

Ji, C., Z. Zhai, C. Jiang, P. Hu, S. Zhao, S. Xue, Z. Yang, T. He, and Q. J. Niu (2021). Recent Advances in High-Performance TFC Membranes: A Review of the Functional Interlayers. *Desalination*, **500**; 114869

Joshi, D. R. and N. Adhikari (2019). An Overview on Common Organic Solvents and Their Toxicity. *Journal of Pharmaceutical Research International*, **28**(3); 1–18

Joshi, R. K., S. Alwarappan, M. Yoshimura, V. Sahajwalla, and Y. Nishina (2015). Graphene Oxide: The New Membrane Material. *Applied Materials Today*, **1**(1); 1–12

Kang, Y., J. Jang, S. Kim, J. Lim, Y. Lee, and I. S. Kim (2020). PIP/TMC Interfacial Polymerization With Electrospray: Novel Loose Nanofiltration Membrane for Dye Wastewater Treatment. *ACS Applied Materials & Interfaces*, **12**(32); 36148–36158

Liu, L., J. Zhang, J. Zhao, and F. Liu (2012). Mechanical Properties of Graphene Oxides. *Nanoscale*, **4**(19); 5910–5916

Marchetti, P., M. F. Jimenez Solomon, G. Szekely, and A. G. Livingston (2014). Molecular Separation With Organic Solvent Nanofiltration: A Critical Review. *Chemical Reviews*, **114**(21); 10735–10806

Naibaho, M., J. Widakdo, B. Kurniawan, P. Z. Z. Nehan, O. Vitayaya, W. A. Adi, and M. Ginting (2024). Analysis of Structure, Morphology, Magnetic Properties, and Microwave Absorption of Lanthanum Orthoferrite ($LaFeO_3$). *Science and Technology Indonesia*, **9**(4); 851–856

Nawi, N. S. M., W. J. Lau, P. S. Goh, J. W. Chew, S. Gray, N. Yusof, and A. F. Ismail (2024). The Impacts of 2D Graphene Oxide on Selective and Substrate Layer of TFC Membrane: A Critical Review on Fabrication Techniques and Performance in Water Treatment. *Journal of Environmental Chemical Engineering*, **12**(2); 112298

Nie, L., C. Y. Chuah, T. H. Bae, and J. M. Lee (2021). Graphene–Based Advanced Membrane Applications in Organic Solvent Nanofiltration. *Advanced Functional Materials*, **31**(6); 2006949

Oguzie, K., E. Oguzie, S. Nwanonenyi, J. Edoziem, and L. Vrsalović (2021). Electrochemical Decolorization of Disperse Blue-1 Dye in Aqueous Solution. *Environmental Engineering & Management Journal (EEMJ)*, **20**(9); 1467–1476

Pan, Z., L. He, L. Qiu, A. H. Korayem, G. Li, J. W. Zhu, F. Collins, D. Li, W. H. Duan, and M. C. Wang (2015). Mechanical Properties and Microstructure of a Graphene Oxide–Cement Composite. *Cement and Concrete Composites*, **58**; 140–147

Qian, Y., C. Zhou, and A. Huang (2018). Cross-Linking Modification With Diamine Monomers to Enhance Desalination Performance of Graphene Oxide Membranes. *Carbon*, **136**; 28–37

Rianjanu, A., S. A. Muhtar, H. F. M. Austria, T. Taher, N. S. Gultom, W. H. Saputera, H. S. Wasisto, F. F. Abdi, W.-S. Hung, and J. Widakdo (2025). 3D Hierarchical Rare-Earth Metal Composite Nanofiber Membranes for Highly Durable and Efficient Photodegradations of Organic Pollutants. *Materials Advances*, **6**(5); 1755–1768

Saeedi, M., B. Malekmohammadi, and S. Tajalli (2024). Interaction of Benzene, Toluene, Ethylbenzene, and Xylene With Human's Body: Insights Into Characteristics, Sources and Health Risks. *Journal of Hazardous Materials Advances*, **16**; 100459

Shen, L., J. Zuo, and Y. Wang (2017). Tris (2-aminoethyl) Amine *In-Situ* Modified Thin-Film Composite Membranes for Forward Osmosis Applications. *Journal of Membrane Science*, **537**; 186–201

Subrahmanya, T., J. Widakdo, S. Mani, H. F. M. Austria, W.-S. Hung, M. HK, J. K. Nagar, C.-C. Hu, and J.-Y. Lai (2022). An Eco-Friendly and Reusable Syringe Filter Membrane for the Efficient Removal of Dyes From Water Via Low Pressure Filtration Assisted Self-Assembling of Graphene Oxide and SBA-15/PDA. *Journal of Cleaner Production*, **349**; 131425

Swan, N. B. and M. A. A. Zaini (2019). Adsorption of Malachite Green and Congo Red Dyes From Water: Recent Progress and Future Outlook. *Ecological Chemistry and Engineering S*, **26**(1); 119–132

Thebo, K. H., X. Qian, Q. Zhang, L. Chen, H.-M. Cheng, and W. Ren (2018). Highly Stable Graphene-Oxide-Based Membranes With Superior Permeability. *Nature Communications*, **9**(1); 1486

Tian, L., N. Graham, T. Liu, K. Sun, and W. Yu (2022). Dual-Site Supported Graphene Oxide Membrane With Enhanced Permeability and Selectivity. *Journal of Membrane Science*, **646**; 120223

Volkov, A. V., V. V. Parashchuk, D. F. Stamatialis, V. S. Khotimsky, V. V. Volkov, and M. Wessling (2009). High Permeable PTMSP/PAN Composite Membranes for Solvent Nanofiltration. *Journal of Membrane Science*, **333**(1-2); 88–93

Wan, X., Y. Huang, and Y. Chen (2012). Focusing on Energy and Optoelectronic Applications: A Journey for Graphene and Graphene Oxide at Large Scale. *Accounts of Chemical Research*, **45**(4); 598–607

Wang, Y.-C., W.-J. Wang, Q. Wang, Z.-Y. Wang, X.-Y. Yan, L.-L. Zhao, X.-L. Cao, and S.-P. Sun (2022). Solvent Remelted Nylon Polyamide Nanofibrous Substrate That Enhances Thin-Film Composite Membranes for Organic Solvent Nanofiltration. *Separation and Purification Technology*, **285**; 120322

Wang, Z., X. Luo, J. Zhang, F. Zhang, W. Fang, and J. Jin (2023). Polymer Membranes for Organic Solvent Nanofiltration: Recent Progress, Challenges and Perspectives. *Advanced Membranes*, **3**; 100063

Wei, J., X. Liu, C. Qiu, R. Wang, and C. Y. Tang (2011). Influence of Monomer Concentrations on the Performance of Polyamide-Based Thin Film Composite Forward Osmosis Membranes. *Journal of Membrane Science*, **381**(1-2); 110–117

Wen, H. and C. Liu (2022). Effect of the Interlayer Construction on the Performances of the TFC-FO Membranes: A Review From Materials Perspective. *Desalination*, **541**; 116033

Widakdo, J., G. T. M. Kadja, A. Anawati, T. Subrahmanya, H. F. M. Austria, T.-H. Huang, E. Suharyadi, and W.-S. Hung (2023). Graphene Oxide-Melamine Nanofilm Composite Membrane for Efficient CO_2 Gas Separation. *Separation and Purification Technology*, **323**; 124521

Wu, L., X. Liu, G. Lv, R. Zhu, L. Tian, M. Liu, Y. Li, W. Rao, T. Liu, and L. Liao (2021). Study on the Adsorption Properties of Methyl Orange by Natural One-Dimensional Nano-Mineral Materials With Different Structures. *Scientific Reports*, **11**(1); 10640

Xiao, H., Y. Feng, W. R. Goundry, and S. Karlsson (2024). Organic Solvent Nanofiltration in Pharmaceutical Applications. *Organic Process Research & Development*, **28**(4); 891–923

Xie, X., Y. Wang, W. Zhou, C. Chen, and Z. Xiong (2021). Investigation of U(VI) Adsorption Properties of Poly (Trime-

soyl Chloride-Co-Polyethyleneimine). *Journal of Solid State Chemistry*, **296**; 121966

Xu, Q., H. Xu, J. Chen, Y. Lv, C. Dong, and T. S. Sreeprasad (2015). Graphene and Graphene Oxide: Advanced Membranes for Gas Separation and Water Purification. *Inorganic Chemistry Frontiers*, **2**(5); 417–424

Xu, Y., F. You, H. Sun, and L. Shao (2017). Realizing Mussel-Inspired Polydopamine Selective Layer With Strong Solvent Resistance in Nanofiltration Toward Sustainable Reclamation. *ACS Sustainable Chemistry & Engineering*, **5**(6); 5520–5528

Yang, Y., G. Li, D. Ouyang, Z. Cai, and Z. Lin (2023). Dual-Activation Interfacial Polymerization Based Anionic Covalent Organic Framework Nanofiltration Membrane for High-Flux Dye Separation. *Chemical Engineering Journal*, **456**; 141008

Zhai, Z., X. Wang, Y. Huang, H. Yang, and Y. Zhao (2023). Fabrication of Advanced Positively Charged Polyamide Nanofiltration Membrane for Effective Removal of Heavy Metal Ions Via Surfactant-Plasticizer-Synergy Assisted Interfacial Polymerization. *Separation and Purification Technology*, **322**(1); 124216

Zhao, S., Z. Zha, C. Mao, Z. Wang, and J. Wang (2022). In-Situ Fabricated Covalent Organic Frameworks-Polyamide Hybrid Membrane for Highly Efficient Molecular Separation. *Journal of Membrane Science*, **653**; 120544

